

Comparison Between Robustified Feedforward and Feedback for Achieving Parameter Robustness

Bong Wie* and Qiang Liu†
Arizona State University, Tempe, Arizona 85281

Both robustified feedforward and feedback control approaches for uncertain dynamical systems (in particular, with uncertainty in structural mode frequency) are investigated. The control objective is to achieve a fast settling time (high performance) and robustness (insensitivity) to plant uncertainty. Preshaping of an ideal, time-optimal control input using a tapped-delay filter is shown to provide a fast settling time with robust performance. A robust, nonminimum-phase feedback controller is synthesized with particular emphasis on its proper implementation for a nonzero set-point control problem. It is shown that a properly designed, feedback controller performs well, as compared with a time-optimal open-loop controller with special preshaping for performance robustness.

I. Introduction

FLEXIBLE structures, including robot manipulators and optical pointing systems in space, are sometimes required to reorient or reposition as quickly as possible with a minimum of residual structural vibrations. The control task for such systems becomes more difficult if they have many flexible modes within the rigid-body control bandwidth. The rapid maneuvering control problem of flexible dynamical systems has been investigated by many researchers, and various feedforward/feedback approaches for minimizing residual structural vibrations have been developed (e.g., see Refs. 1-9).

The basic idea behind the various feedforward approaches is to find an input forcing function (e.g., such as a versine function) that begins and ends with zero slope so that structural modes are less likely to be excited. Such an input function, however, does not fully utilize the available maximum maneuvering force, and results in a slower response time and also residual structural vibrations. Most feedforward approaches (in particular, an open-loop optimal approach) require accurate modeling of the system and thus are not robust to plant modeling uncertainty. Recently, Singer and Seering^{7,8} have developed an alternative, robust approach of shaping a feedforward input command by acausally filtering out the frequency components of flexible mode resonances. Some tradeoffs, however, must be made between performance (a fast settling time) and robustness (insensitivity) to plant parameter uncertainty even for this preshaped open-loop approach.

This paper provides a comparison between a preshaped feedforward command generator^{7,8} and a robustified feedback controller¹⁰⁻¹³ with nonzero set-point command for a reference-input tracking problem. It is, however, emphasized that one of the primary motivations for the use of closed-loop rather than open-loop control systems in practice is to cope with unexpected disturbances, which an open-loop controller cannot. Such a disturbance rejection problem is not considered in this paper. A simple generic model of uncertain dy-

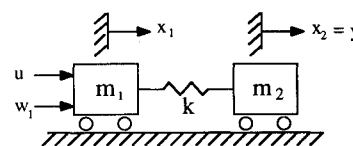


Fig. 1 Two-mass spring example.

namical systems shown in Fig. 1 is used to illustrate the control concepts and methodologies.

The remainder of this paper is organized as follows. In Sec. II, time-optimal control inputs are determined for this example problem. In Sec. III, such time-optimal control inputs are preshaped using a tapped-delay filter to provide a rapid maneuver and robust suppression of residual structural vibrations. A robust H_∞ compensator design is discussed in Sec. IV, with special emphasis on a proper implementation of a nonminimum-phase compensator for a nonzero set-point control problem. It will be shown that a properly designed, feedback controller performs well, as compared with a time-optimal open-loop controller with special preshaping for parameter robustness.

II. Time-Optimal Control

Consider a generic example of flexible dynamical systems as shown in Fig. 1. It is assumed that the two bodies both have nominal unit mass ($m_1 = m_2 = 1$) and are connected by a spring with nominal stiffness $k = 1$. A control input force u acts on body 1 and the position of body 2 is the output to be controlled ($y = x_2$). It is assumed that the control input is bounded as $|u| \leq 1$.

In this section, time-optimal, open-loop control input $u(t)$ is determined by minimizing the performance index

$$J = \int_0^{t_f} dt = t_f \quad (1)$$

where t_f is the final time to be determined. The resulting time-optimal control input will be preshaped in Sec. III, using a tapped-delay filter, to improve performance robustness with respect to plant parameter uncertainty.

Rigid-Body Time-Optimal Control

For a "rigidized" model of the nominal system shown in Fig. 1, the equation of motion is simply

$$(m_1 + m_2)\ddot{y} = u \quad (2)$$

Received June 22, 1990; presented as Paper 90-3424 at the AIAA Guidance, Navigation, and Control Conference, Portland, OR, Aug. 20-22, 1990; revision received Dec. 13, 1990; accepted for publication Jan. 28, 1991. Copyright © 1990 by the American Institute of Aeronautics and Astronautics, Inc. All rights reserved.

*Associate Professor, Department of Mechanical and Aerospace Engineering. Member AIAA.

†Graduate Research Assistant. Student Member AIAA.

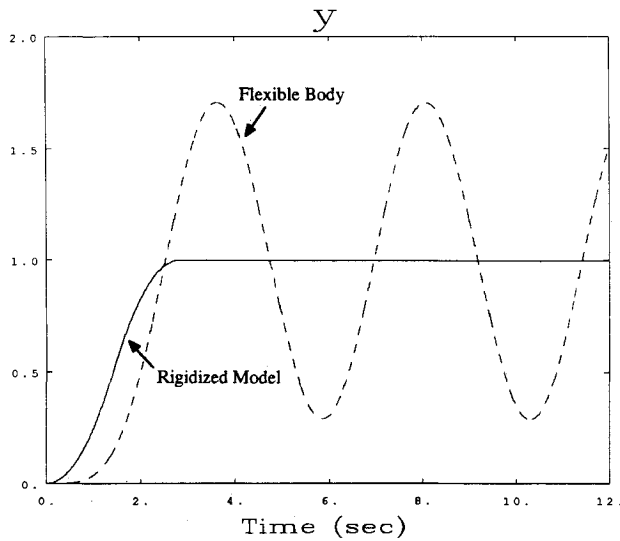


Fig. 2 Responses to rigid-body, time-optimal control input.

The rest-to-rest, time-optimal solution for $y(0) = 0$ and $y(t_f) = 1$ can be found as

$$u(t) = u_s(t) - 2u_s[t - (t_f/2)] + u_s(t - t_f) \quad (3)$$

where $t_f = 2\sqrt{(m_1 + m_2)y(t_f)} = 2.828$ s and $u_s(t)$ represents a unit-step function.

If this time-optimal input force is exerted on the nominal system with a flexible mode (Fig. 1), a significant residual structural vibration will occur, as can be seen in Fig. 2.

Flexible-Body Time-Optimal Control

Consider a time-optimal control problem for the flexible-body model shown in Fig. 1. The equations of motion are

$$m_1\ddot{x}_1 + k(x_1 - x_2) = u \quad (4a)$$

$$m_2\ddot{x}_2 - k(x_1 - x_2) = 0 \quad (4b)$$

where x_1 and x_2 are the positions of body 1 and body 2, respectively. This system can also be represented in state-space form as

$$\dot{x}(t) = Ax(t) + Bu(t) \quad (5)$$

where

$$x = [x_1 \ x_2 \ \dot{x}_1 \ \dot{x}_2]^T, \quad A = \begin{bmatrix} 0 & 0 & 1 & 0 \\ 0 & 0 & 0 & 1 \\ -k/m_1 & k/m_1 & 0 & 0 \\ k/m_2 & -k/m_2 & 0 & 0 \end{bmatrix}$$

$$B = \begin{bmatrix} 0 \\ 0 \\ 1/m_1 \\ 0 \end{bmatrix}$$

The time-optimal control input for this problem, which first appeared in Ref. 10, can be solved using the following approach discussed in Ref. 4. For our two-mass-spring model, three switching times are required. The nominal system with $m_1 = m_2 = k = 1$ is first transformed into modal equations by

the coordinate transformation

$$\begin{bmatrix} x_1 \\ x_2 \end{bmatrix} = \begin{bmatrix} 1 & 1 \\ 1 & -1 \end{bmatrix} \begin{bmatrix} q_1 \\ q_2 \end{bmatrix} \quad (6)$$

where q_1 and q_2 are the modal coordinates, and the resulting modal equations are

$$\ddot{q}_1 = u/2 \quad (7a)$$

$$\ddot{q}_2 + \omega^2 q_2 = u/2 \quad (7b)$$

where $\omega = \sqrt{2}$ rad/s is the nominal flexible mode frequency. For given boundary conditions

$$q_1(0) = 0, \quad \dot{q}_1(0) = 0$$

$$q_2(0) = 0, \quad \dot{q}_2(0) = 0$$

$$q_1(t_f) = 1, \quad \dot{q}_1(t_f) = 0$$

$$q_2(t_f) = 0, \quad \dot{q}_2(t_f) = 0$$

the following two-constraints can be obtained as

$$1 - 2 \cos \omega t_1 + 2 \cos \omega t_2 - 2 \cos \omega t_3 + \cos \omega t_f = 0$$

$$4 - t_f^2 + 2(t_f - t_1)^2 - 2(t_f - t_2)^2 + 2(t_f - t_3)^2 = 0$$

where t_1 , t_2 , and t_3 are the switching times and t_f the final time to be solved. From the symmetric nature of this problem, we have

$$t_2 = t_f/2, \quad t_1 = t_f - t_3$$

and the switching times can be found as $t_1 = 1.00268$ s, $t_2 = 2.10893$ s, $t_3 = 3.21518$ s, and $t_f = 4.21786$ s. Note that a longer maneuver time of 4.217 s is required for a flexible body, as compared with the maneuver time of 2.828 s for a rigidized system.

The time-optimal control input can then be expressed as

$$u(t) = u_s(t) - 2u_s(t - t_1) + 2u_s(t - t_2) - 2u_s(t - t_3) + u_s(t - t_f) \quad (8)$$

The open-loop responses of the system to this time-optimal control input are shown in Fig. 3 for four different values of k . It can be seen that an ideal, minimum-time maneuver is achieved for the nominal system and that perturbations in spring constant k , however, result in residual vibrations of the flexible mode.

III. Preshaped Time-Optimal Control

As shown in the preceding section, the time-optimal solution requires accurate modeling of the system, and the open-loop responses to such an ideal input force are very sensitive to the plant modeling uncertainty. In this section, an "impulse-sequence" shaping technique developed by Singer and Seering^{7,8} is employed to preshape the ideal, time-optimal inputs. Performance of the resulting robust feedforward controller will be compared with that of a robust feedback controller in Sec. IV.

The preshaping technique in Refs. 7 and 8 simply utilizes a tapped-delay filter with proper weightings and time delays. This technique is briefly reviewed here for our example with a single, undamped flexible mode.

A sequence of m impulses can be expressed in time domain as

$$f(t) = \sum_{i=1}^m A_i \delta(t - t_i) \quad (9)$$

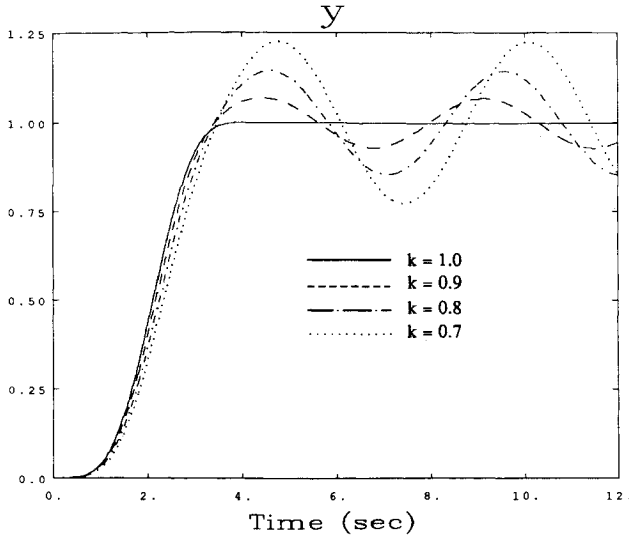


Fig. 3 Responses to flexible-body, time-optimal control input.

with the following normalization

$$\sum_{i=1}^m A_i = 1 \quad (10)$$

where A_i is the magnitude of the i th impulse at $t = t_i$ and the last impulse occurs at $t = t_m$.

A bang-bang function with $(n-2)$ switches can be represented as

$$u(t) = \sum_{j=1}^n B_j u_s(t - t_j) \quad (11)$$

where B_j is the magnitude of a step function at $t = t_j$. This bang-bang function ends at $t = t_n$.

The convolution of $u(t)$ and $f(t)$ will result in a new multi-switch, multilevel, bang-bang function

$$\tilde{u}(t) = \sum_{i=1}^n \sum_{j=1}^m A_i B_j u_s(t - t_i - t_j) \quad (12)$$

This function has $(mn-2)$ switching times and ends at $t = (t_m + t_n)$.

A proper sequence of impulses, whose power spectrum has a notch at a structural resonant frequency, can be found as follows. If a sequence of m impulses in Eq. (9) is applied to an undamped second-order system with a natural frequency of ω , the system response for $t > t_m$ can be represented as

$$\sum_{i=1}^m A_i \omega \sin \omega(t - t_i) = A \sin(\omega t - \phi) \quad (13)$$

where

$$A = \sqrt{\left(\sum_{i=1}^m A_i \omega \cos \omega t_i \right)^2 + \left(\sum_{i=1}^m A_i \omega \sin \omega t_i \right)^2}$$

$$\phi = \tan^{-1} \left(\frac{\sum_{i=1}^m A_i \sin \omega t_i}{\sum_{i=1}^m A_i \cos \omega t_i} \right)$$

If A_i and t_i are chosen such that $A = 0$, that is,

$$A_1 \cos \omega t_1 + A_2 \cos \omega t_2 + \cdots + A_m \cos \omega t_m = 0 \quad (14a)$$

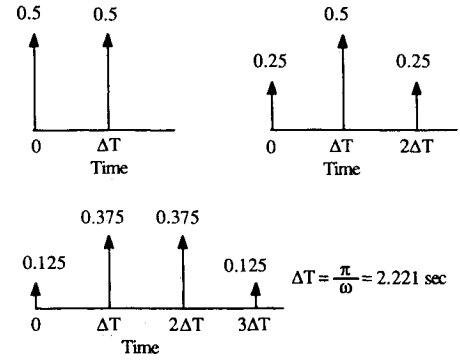


Fig. 4 Impulse-sequence shaping.

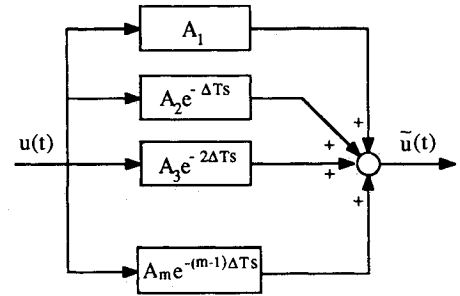


Fig. 5 Tapped-delay filter.

$$A_1 \sin \omega t_1 + A_2 \sin \omega t_2 + \cdots + A_m \sin \omega t_m = 0 \quad (14b)$$

then the residual vibration will not occur after $t = t_m$.

Taking derivatives of the preceding two equations for $(m-2)$ times with respect to ω , we get the following $2(m-2)$ robustness constraint equations

$$A_1(t_1)^j \sin \omega t_1 + A_2(t_2)^j \sin \omega t_2 + \cdots + A_m(t_m)^j \sin \omega t_m = 0 \quad (15a)$$

$$A_1(t_1)^j \cos \omega t_1 + A_2(t_2)^j \cos \omega t_2 + \cdots + A_m(t_m)^j \cos \omega t_m = 0 \quad (15b)$$

where $j = 1, \dots, m-2$. For an m -impulse sequence with $t_1 = 0$, we now have $(2m-1)$ equations for $(2m-1)$ unknowns.

Figure 4 illustrates three different impulse sequences with proper A_i and the time-delay interval of $\Delta T = \pi/\omega$, where ω is the natural frequency of the flexible mode under consideration.

The frequency-response characteristics of this impulse-sequence shaping technique can be analyzed simply by taking the Laplace transform of an m -impulse sequence as follows:

$$\begin{aligned} \mathcal{L}[f(t)] &= \sum_{i=1}^m A_i e^{-t_i s} \\ &= \sum_{i=1}^m A_i e^{-\Delta T(i-1)s} \end{aligned} \quad (16)$$

which can be interpreted as a tapped-delay filter (see Fig. 5). The frequency responses of this tapped-delay filter for $m = 2, 3$, and 4 are shown in Fig. 6. It can be seen that the frequency component around the resonant frequency is notched out. The wider notch width indicates more robustness to frequency uncertainty, but a longer response time.

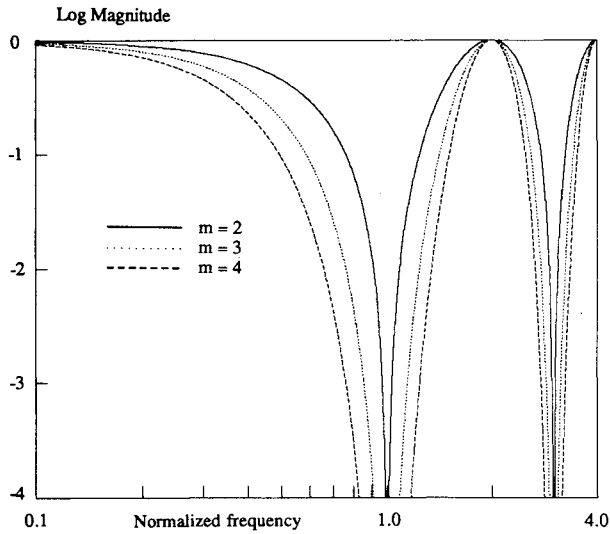


Fig. 6 Frequency responses of tapped-delay filter with $m = 2, 3, 4$.

The flexible-body time-optimal input given by Eq. (8) is now preshaped by a tapped-delay filter with $m = 2$, resulting in the preshaped input command

$$\begin{aligned} \bar{u}(t) = & 0.5u_s(t) - u_s(t - 1.003) + u_s(t - 2.109) \\ & + 0.5u_s(t - 2.221) - u_s(t - 3.215) - u_s(t - 3.224) \\ & + 0.5u_s(t - 4.218) + u_s(t - 4.330) + u_s(t - 5.436) \\ & + 0.5u_s(t - 6.439) \end{aligned} \quad (17)$$

This preshaped input takes values of ± 1.0 and ± 0.5 .

The flexible-body time-optimal input is also preshaped using a tapped-delay filter with $m = 3$, resulting in the preshaped control input command

$$\begin{aligned} \bar{u}(t) = & 0.25u_s(t) - 0.5u_s(t - 1.003) + 0.5u_s(t - 2.109) \\ & + 0.5u_s(t - 2.221) - 0.5u_s(t - 3.215) - u_s(t - 3.224) \\ & + 0.25u_s(t - 4.218) + u_s(t - 4.330) + 0.25u_s(t - 4.442) \\ & - u_s(t - 5.436) - 0.5u_s(t - 5.445) + 0.5u_s(t - 6.439) \\ & + 0.5u_s(t - 6.551) + 0.5u_s(t - 7.657) \\ & + 0.25u_s(t - 8.660) \end{aligned} \quad (18)$$

It can be seen from Fig. 7 that the preshaped command takes values of $\pm 0.25, \pm 0.5, \pm 0.75$. The time responses of the system to this preshaped input are shown in Fig. 8 for four different values of k . It is evident that robustness with respect to flexible mode frequency has been increased at the expense of increased maneuver time to about 8.66 s, comparing with the ideal minimum time of 4.218 s shown in Fig. 3.

The simple, rigid-body time-optimal input given by Eq. (3) can also be preshaped to reduce the residual vibration shown in Fig. 2. For example, preshaping the rigid-body bang-bang command with a tapped-delay filter with $m = 3$ results in another bang-bang command:

$$\begin{aligned} u(t) = & 0.25u_s(t) - 0.5u_s(t - 1.414) + 0.5u_s(t - 2.221) \\ & + 0.25u_s(t - 2.828) - u_s(t - 3.635) + 0.25u_s(t - 4.442) \\ & + 0.5u_s(t - 5.049) - 0.5u_s(t - 5.856) + 0.25u_s(t - 7.270) \end{aligned} \quad (19)$$

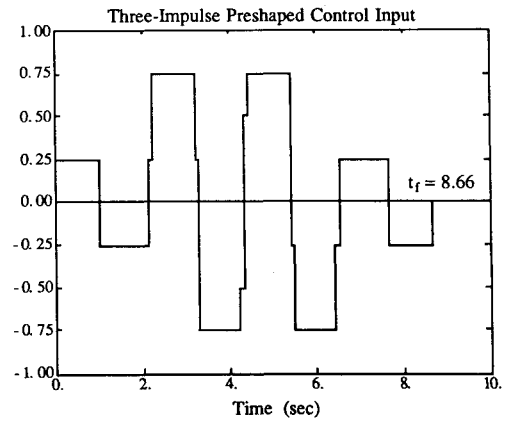


Fig. 7 Flexible-body, time-optimal command, preshaped with tapped-delay filter with $m = 3$.

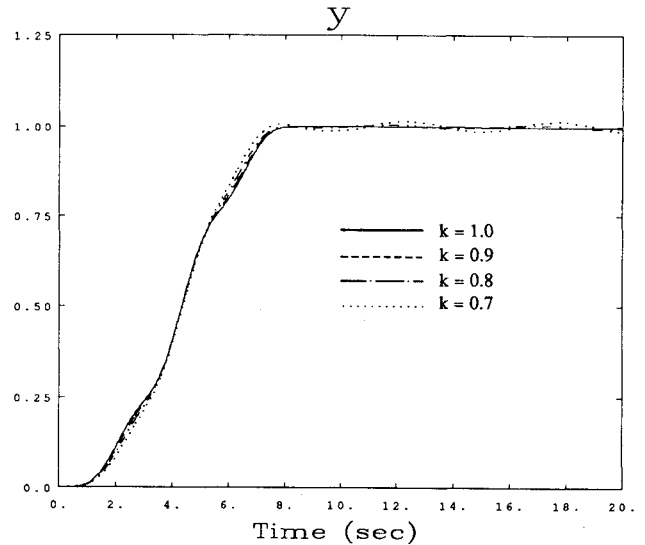


Fig. 8 Responses to preshaped time-optimal command.

The responses of the system to this preshaped input (not shown here) also indicate a reasonable performance robustness (but not better than Fig. 8). In practice, however, the time-optimal solution for a rigidized rather than flexible model of a multilink flexible robot (e.g., see Ref. 14) may be preshaped using a tapped-delay filter to accommodate the flexible mode effects.

In summary, we have shown that time-optimal control input, preshaped using a tapped delay filter, provides a robust maneuvering scheme that can minimize residual structural vibrations. It is also evident that some tradeoffs between performance and robustness must always be considered. In the next section, a robust feedback compensator will be designed and its performance and robustness will be compared with that of the robust, preshaped feedforward approach discussed in this section.

IV. Robust Feedback Control Design

As discovered in Refs. 10–13 a nonminimum-phase compensation is particularly useful for practical tradeoffs between performance and robustness for a certain class of noncollocated structural control problems. It is, however, often criticized because of its sluggish response and its loop gain limitation. In this section, a robust H_∞ feedback compensator design is discussed with special emphasis on a proper implementation of a nonminimum-phase compensator, incorporating a nonzero set-point control scheme. It is shown that a properly designed, feedback controller with a nonzero set-

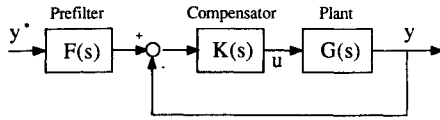


Fig. 9 Conventional feedforward/feedback control system configuration.

point command performs well, as compared with a time-optimal, open-loop controller with special pre shaping for robustness.

Consider a single-input single-output (SISO) control system as illustrated in Fig. 9, which is the most commonly used configuration for a "two-degree-of-freedom" controller. The plant and compensator transfer functions are represented as

$$K(s) = N_c(s)/D_c(s) \quad (20a)$$

$$G(s) = N(s)/D(s) \quad (20b)$$

where $N_c(s)$, $D_c(s)$, $N(s)$, and $D(s)$ are polynomials of the Laplace transform variable s . The closed-loop transfer function from the desired output command y^* to the actual output y is then

$$\begin{aligned} \frac{y(s)}{y^*(s)} &= \frac{K(s)G(s)}{1 + K(s)G(s)} F(s) \\ &= \frac{N_c(s)N(s)}{D_c(s)D(s) + N_c(s)N(s)} F(s) \end{aligned} \quad (21)$$

Thus, for the conventional feedback control system of Fig. 9, the zeros of the closed-loop transfer function are identical with the zeros of the loop transfer function $K(s)G(s)$. These zeros sometimes cause an excessive, transient peak overshoot even when the closed-loop poles are properly selected. In this case, a prefilter $F(s)$ is often used for the cancellation of the undesirable zeros of the closed-loop transfer function. (Of course, we cannot cancel the nonminimum-phase zeros!)

If the compensator is placed in the feedback path, the closed-loop transfer function becomes

$$\begin{aligned} \frac{y(s)}{y^*(s)} &= \frac{G(s)}{1 + K(s)G(s)} F(s) \\ &= \frac{D_c(s)N(s)}{D_c(s)D(s) + N_c(s)N(s)} F(s) \end{aligned} \quad (22)$$

where the compensator zeros do not appear as zeros of the closed-loop transfer function, and a prefilter $F(s)$ must be properly designed for the generation of a control input command. Recall that one of the primary motivations for the use of closed-loop rather than open-loop control systems in practice is to cope with unexpected disturbances, which an open-loop controller cannot. For this reason, feedforward control is seldom used alone, but rather, it is used in combination with feedback control.

In this section, we show a proper way of implementing a nonminimum-phase compensator to minimize such excessive, transient peak overshoot caused by the compensator zeros. We briefly review a robust H_∞ control design methodology developed in Refs. 12 and 13, and we present a nonzero set-point control scheme for an H_∞ -based controller, followed by an example design.

Robust H_∞ Control

Consider a linear, time-invariant system described by

$$\dot{x}(t) = Ax(t) + B_1 w(t) + B_2 u(t) \quad (23a)$$

$$z(t) = C_1 x(t) + D_{11} w(t) + D_{12} u(t) \quad (23b)$$

$$y(t) = C_2 x(t) + D_{21} w(t) + D_{22} u(t) \quad (23c)$$

where $x(t)$ is an n -dimensional state vector, $w(t)$ an m_1 -dimensional disturbance vector, $u(t)$ an m_2 -dimensional control vector, $z(t)$ a p_1 -dimensional controlled output vector, and $y(t)$ a p_2 -dimensional measurement vector.

To utilize the concept of an internal feedback loop, the system with uncertain parameters is described as^{12,13}

$$\begin{bmatrix} \dot{x} \\ z \\ y \end{bmatrix} = \begin{bmatrix} \hat{A} & \hat{B}_1 & \hat{B}_2 \\ C_1 & D_{11} & D_{12} \\ \hat{C}_2 & \hat{D}_{21} & \hat{D}_{22} \end{bmatrix} \begin{bmatrix} x \\ w \\ u \end{bmatrix} \quad (24)$$

where C_1 , D_{11} , and D_{12} are not subject to parameter variations. The perturbed system matrix in Eq. (24) can be linearly decomposed as follows:

$$\begin{bmatrix} \dot{x} \\ z \\ y \end{bmatrix} = \left\{ \begin{bmatrix} A & B_1 & B_2 \\ C_1 & D_{11} & D_{12} \\ C_2 & D_{21} & D_{22} \end{bmatrix} + \Delta_p \right\} \begin{bmatrix} x \\ w \\ u \end{bmatrix} \quad (25)$$

where the first matrix in the right-hand side is the nominal system matrix and Δ_p is the perturbation matrix defined as

$$\Delta_p \triangleq \begin{bmatrix} \Delta A & \Delta B_1 & \Delta B_2 \\ 0 & 0 & 0 \\ \Delta C_2 & \Delta D_{21} & \Delta D_{22} \end{bmatrix} \quad (26)$$

Suppose that there are l independent perturbed parameters p_1, \dots, p_l which are bounded as $|\Delta p_i| \leq 1$. The perturbation matrix Δ_p is then decomposed with respect to each parameter variation as

$$\Delta_p = - \begin{bmatrix} M_x \\ 0 \\ M_y \end{bmatrix} E [N_x \ N_w \ N_u] = -MEN \quad (27)$$

where

$$E = \begin{bmatrix} \Delta p_1 & & 0 \\ & \ddots & \\ 0 & & \Delta p_l \end{bmatrix} \quad (28)$$

By introducing the following new variables

$$z_p \triangleq [N_x \ 0 \ N_w \ N_u] \begin{bmatrix} x \\ w_p \\ w \\ u \end{bmatrix} \quad (29a)$$

$$w_p \triangleq -E z_p \quad (29b)$$

the perturbed system, Eq. (25), and the input-output decomposition, Eq. (27), can be combined as

$$\begin{bmatrix} \dot{x} \\ z_p \\ z \\ y \end{bmatrix} = \begin{bmatrix} A & M_x & B_1 & B_2 \\ N_x & 0 & N_w & N_u \\ C_1 & 0 & D_{11} & D_{12} \\ C_2 & M_y & D_{21} & D_{22} \end{bmatrix} \begin{bmatrix} x \\ w_p \\ w \\ u \end{bmatrix} \quad (30a)$$

$$w_p = -E z_p \quad (30b)$$

where w_p and z_p are considered as the fictitious input and output, respectively, due to the plant perturbation; and E is considered as a fictitious, internal feedback loop gain matrix.

The following redefinition of z , w , and expansion of the associated matrices enable us to employ the state-space representation given by Eq. (23):

$$\begin{aligned} z &\leftarrow \begin{bmatrix} z_p \\ z \end{bmatrix}, \quad w \leftarrow \begin{bmatrix} w_p \\ w \end{bmatrix}, \quad B_1 \leftarrow [M_x \ B_1], \quad C_1 \leftarrow \begin{bmatrix} N_x \\ C_1 \end{bmatrix} \\ D_{11} &\leftarrow \begin{bmatrix} 0 & N_w \\ 0 & D_{11} \end{bmatrix}, \quad D_{12} \leftarrow \begin{bmatrix} N_u \\ D_{12} \end{bmatrix}, \quad D_{21} \leftarrow [M_y \ D_{21}] \end{aligned} \quad (31)$$

It can be shown that under certain conditions, there exists an internally stabilizing controller such that, for the closed-loop transfer matrix T and for a given design variable γ ,

$$\|T\|_{\infty} < \gamma$$

if and only if the following Riccati equations¹⁵

$$0 = A^T X + X A - X(B_2 B_2^T - \frac{1}{\gamma^2} B_1 B_1^T)X + C_1^T C_1 \quad (32)$$

$$0 = A Y + Y A^T - Y(C_2^T C_2 - \frac{1}{\gamma^2} C_1^T C_1)Y + B_1 B_1^T \quad (33)$$

have unique symmetric positive semidefinite solutions X and Y .

An H_{∞} -suboptimal controller that satisfies $\|T_{zw}\|_{\infty} < \gamma$, where γ is a design variable specifying an upper bound of the perturbed closed-loop performance T_{zw} , is then obtained as

$$u(s) = -K[sI - A_c]^{-1} L y(s) \quad (34)$$

or

$$\dot{x}_c = A_c x_c + L y \quad (35a)$$

$$u = -K x_c \quad (35b)$$

where

$$K = B_2^T X \quad (36a)$$

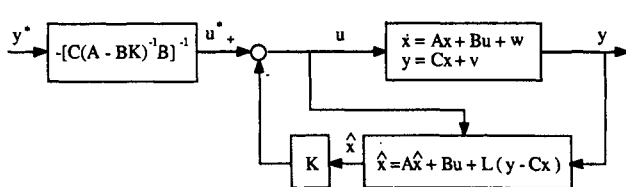


Fig. 10 Control system configuration with LQG-type controller.

$$L = \left(I - \frac{1}{\gamma^2} Y X\right)^{-1} Y C_2^T \quad (36b)$$

$$A_c = A + \frac{1}{\gamma^2} B_1 B_1^T X - B_2 K - L C_2 \quad (36c)$$

Note that this H_{∞} controller has a structure similar to a conventional state-space controller consisting of an estimator and a regulator, but is designed for a plant system matrix

$$A + \frac{1}{\gamma^2} B_1 B_1^T X$$

where $B_1 B_1^T X / \gamma^2$ can be interpreted as an estimate for the worst disturbance input. In other words, the separation principle of the conventional linear-quadratic-Gaussian (LQG) technique does not hold here. Consequently, the nonzero set-point control scheme, which has been well-established for LQG control synthesis, needs some minor modification as discussed in the next section.

Nonzero Set-Point Control

A block diagram representation of a SISO closed-loop system for a conventional LQG-type controller with a nonzero set-point command is illustrated in Fig. 10. For this configuration, the control input command u^* corresponding to the desired (constant) output command y^* is simply given as

$$u^* = -[C(A-BK)^{-1}B]^{-1} y^* \quad (37)$$

which is independent of the estimator gain matrix L . In this case, we can easily show that for dynamic systems having a rigid-body mode, u^* depends only on the regulator parameters (not on the plant parameters such as m_1 , m_2 , and k of the example model shown in Fig. 1). Hence, the nonzero set-point control scheme is inherently robust to plant parameter uncertainty for a certain class of dynamical systems with at least one pole at the origin (i.e., a type-1 system).

Now consider a closed-loop control system with an H_{∞} controller as shown in Fig. 11, which is described in state-space form as

$$\begin{bmatrix} \dot{x} \\ \dot{x}_c \end{bmatrix} = \begin{bmatrix} A & -B_2 K \\ L C_2 & A_c \end{bmatrix} \begin{bmatrix} x \\ x_c \end{bmatrix} + \begin{bmatrix} B_2 \\ B_2 \end{bmatrix} u^* \quad (38a)$$

$$y = [C_2 \ 0] \begin{bmatrix} x \\ x_c \end{bmatrix} \quad (38b)$$

The input command u^* corresponding to the desired output y^* can be simply found as

$$u^* = -[\bar{C}\bar{A}^{-1}\bar{B}]^{-1} y^* \quad (39)$$

where

$$\bar{A} = \begin{bmatrix} A & -B_2 K \\ L C_2 & A_c \end{bmatrix}, \quad \bar{B} = \begin{bmatrix} B_2 \\ B_2 \end{bmatrix}, \quad \bar{C} = [C_2 \ 0] \quad (40)$$

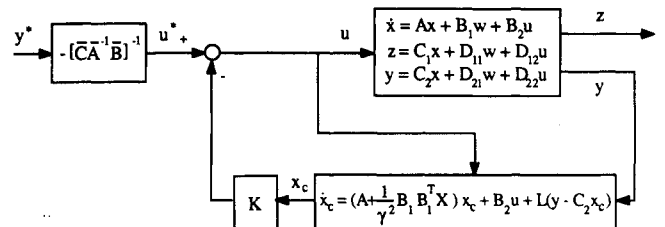


Fig. 11 Control system configuration with H_{∞} -type controller.

Similar to the LQG case, it can be shown that for dynamic systems having a rigid-body mode, u^* for an H_∞ controller depends only on the controller parameters (not on the plant parameters such as m_1 , m_2 , and k of the example model shown in Fig. 1). However, u^* now depends on both the gain matrices K and L , not just on the regulator gain matrix K as for the LQG case.

Example Design

We now consider the two-mass spring model shown in Fig. 1. A control input force u acts on body 1 and the position of body 2 is measured as y , resulting in the so-called noncollocated control problem. The control design objective here is to achieve a fast settling time (high performance) for an output command $y^* = 1$ and robust performance over a range of spring stiffness uncertainty considered in Sec. III. The control input is bounded as $|u| \leq 1$ and the system has the nominal values of $m_1 = m_2 = k = 1$.

The plant model can be represented in state-space form as

$$\begin{bmatrix} \dot{x}_1 \\ \dot{x}_2 \\ \dot{x}_3 \\ \dot{x}_4 \end{bmatrix} = \begin{bmatrix} 0 & 0 & 1 & 0 \\ 0 & 0 & 0 & 1 \\ -k & k & 0 & 0 \\ k & -k & 0 & 0 \end{bmatrix} \begin{bmatrix} x_1 \\ x_2 \\ x_3 \\ x_4 \end{bmatrix} + \begin{bmatrix} 0 \\ 0 \\ 1 \\ 0 \end{bmatrix} (u + w_1) \quad (41a)$$

$$y = x_2 + v \quad (41b)$$

$$z = x_2 \quad (41c)$$

where w_1 and v are, respectively, plant disturbance and sensor noise assumed for control design purposes.

The variation ΔA is decomposed as

$$\Delta A = -\Delta k \begin{bmatrix} 0 \\ 0 \\ 1 \\ -1 \end{bmatrix} [1 \ -1 \ 0 \ 0] \quad (42)$$

The other elements of the perturbation matrix in Eq. (26) are all zeros. Note that ΔA is spanned by the matrices

$$M_x = \begin{bmatrix} 0 \\ 0 \\ 1 \\ -1 \end{bmatrix}, \quad N_x = [1 \ -1 \ 0 \ 0]$$

where M_x is the fictitious disturbance distribution matrix spanning the columns of ΔA , and N_x is the fictitious-controlled output distribution matrix spanning the rows of ΔA . The fictitious input and output for this example are expressed as

$$z_p = N_x x = x_1 - x_2, \quad w_p = -\Delta k z_p \quad (43)$$

Equation (43) replaces the parameter variation in Eq. (41), resulting in the following equations:

$$\begin{bmatrix} \dot{x}_1 \\ \dot{x}_2 \\ \dot{x}_3 \\ \dot{x}_4 \end{bmatrix} = \begin{bmatrix} 0 & 0 & 1 & 0 \\ 0 & 0 & 0 & 1 \\ -k & k & 0 & 0 \\ k & -k & 0 & 0 \end{bmatrix} \begin{bmatrix} x_1 \\ x_2 \\ x_3 \\ x_4 \end{bmatrix} + \begin{bmatrix} 0 \\ 0 \\ 1 \\ 0 \end{bmatrix} (u + w_1)$$

$$+ \begin{bmatrix} 0 \\ 0 \\ 1 \\ 0 \end{bmatrix} (u + w_1) + \begin{bmatrix} 0 \\ 0 \\ 1 \\ -1 \end{bmatrix} w_p \quad (44a)$$

$$\begin{bmatrix} z_p \\ z \end{bmatrix} = \begin{bmatrix} x_1 - x_2 \\ x_2 \\ u \end{bmatrix} \quad (44b)$$

$$y = x_2 + v \quad (44c)$$

where k is the nominal spring constant. As can be seen in Eq. (44b), control input u is also included in the performance variable z in order to minimize control effort.

By defining

$$w = \begin{bmatrix} w_p \\ w_1 \\ v \end{bmatrix}, \quad z = \begin{bmatrix} z_p \\ z \end{bmatrix} \quad (45)$$

and by using the definition of Eq. (31), the system matrices in Eq. (23) can be represented as

$$A = \begin{bmatrix} 0 & 0 & 1 & 0 \\ 0 & 0 & 0 & 1 \\ -k & k & 0 & 0 \\ k & -k & 0 & 0 \end{bmatrix}, \quad B_1 = \begin{bmatrix} 0 & 0 & 0 \\ 0 & 0 & 0 \\ 1 & 1 & 0 \\ -1 & 0 & 0 \end{bmatrix}$$

$$B_2 = \begin{bmatrix} 0 \\ 0 \\ 1 \\ 0 \end{bmatrix}, \quad C_1 = \begin{bmatrix} 1 & -1 & 0 & 0 \\ 0 & 1 & 0 & 0 \\ 0 & 0 & 0 & 0 \end{bmatrix}, \quad D_{12} = \begin{bmatrix} 0 \\ 0 \\ 1 \end{bmatrix}$$

$$C_2 = [0 \ 1 \ 0 \ 0], \quad D_{21} = [0 \ 0 \ 1] \quad (46)$$

and $D_{11} = 0_{3 \times 3}$, $D_{22} = 0$.

For the example design considered here, the disturbances w_p , w_1 , and v are multiplied by weighting factors 0.1, 0.025, and 0.025, respectively. The performance specification bound γ is chosen to be 1. The weighting factors and γ represent relative disturbance levels and overall closed-loop performance level, respectively.

By solving two Riccati equations, Eqs. (32) and (33), we get the controller gain matrices K and L as follows:

$$K = [1.506 \ -0.494 \ 1.738 \ 0.932]$$

$$L = [0.720 \ 2.973 \ -3.370 \ 4.419]^T$$

The corresponding H_∞ controller is then

$$u(s) = -\frac{0.827(s/0.145 + 1)(-s/0.984 + 1)}{[(s/1.586)^2 + 2(0.825)(s/1.586) + 1]} \times \frac{(s/3.434 + 1)}{[(s/2.240)^2 + 2(0.459)(s/2.240) + 1]} y(s) \quad (47)$$

⁵Meckl, P. H., and Seering, W. P., "Minimizing Residual Vibration for Point-to-Point Motion," *Journal of Vibration, Acoustics, Stress and Reliability in Design*, Vol. 107, Oct. 1985, pp. 378-382.

⁶Meckl, P. H., and Seering, W. P., "Feedforward Control Techniques to Achieve Fast Settling Time in Robots," *Proceedings of the American Control Conference*, Seattle, WA, June 1986, pp. 1913-1918.

⁷Singer, N. C., and Seering, W. P., "Using Acausal Shaping Techniques to Achieve Fast Settling Time in Robots," *Proceedings of the 1988 IEEE International Conference On Robotics and Automation*, Philadelphia, PA, April 25-29, 1988, pp. 1434-1437.

⁸Singer, N. C., and Seering, W. P., "Preshaping Command Inputs to Reduce System Vibration," *Proceedings of the 1989 IEEE International Conference on Robotics and Automation*, Scottsdale, AZ, May 1989, pp. 888-893.

⁹Byers, R. M., Vadali, S. R., and Junkins, J. L., "Near-Minimum Time, Closed-Loop Slewing of Flexible Spacecraft," *Journal of Guidance, Control, and Dynamics*, Vol. 13, No. 1, 1990, pp. 57-65.

¹⁰Bryson, A. E., Jr., Hermelin, S., and Sun, J., "LQG Controller Design for Robustness," American Control Conf., Seattle, WA,

June, 1986.

¹¹Wie, B., and Byun, K.-W., "New Generalized Structural Filtering Concept for Active Vibration Control Synthesis," *Journal of Guidance, Control, and Dynamics*, Vol. 12, No. 2, 1989, pp. 147-154.

¹²Byun, K.-W., Wie, B., and Sunkel, J., "Robust Nonminimum-Phase Compensation for a Class of Uncertain Dynamical Systems," *Journal of Guidance, Control, and Dynamics*, Vol. 14, No. 6, 1991, pp. 1191-1199.

¹³Wie, B., Liu, Q., and Byun, K.-W., "Robust H_∞ Control Design Method and Its Application to a Benchmark Problem," 1990 American Control Conf., San Diego, CA, May 1990; *Journal of Guidance, Control, and Dynamics* (to be published).

¹⁴Wie, B., Chuang, C.-H., and Sunkel, J., "Minimum-Time Pointing Control of a Two-Link Manipulator," *Journal of Guidance, Control, and Dynamics*, Vol. 13, No. 5, 1990, pp. 867-873.

¹⁵Doyle, J., Glover, K., Khargonekar, P., and Francis, B., "State-Space Solutions to Standard H_2 and H_∞ Control Problems," *IEEE Transactions on Automatic Control*, Vol. 34, No. 8, 1989, pp. 831-847.